

University of Massachusetts Amherst

From the Selected Works of Ajla Aksamija

2018

Thermoelectric Materials in Exterior Walls: Experimental Study on Using Smart Facades for Heating and Cooling in High-Performance Buildings

Dr. Ajla Aksamija, *University of Mass*

Zlatan Aksamija

Christopher H Counihan

Dylan Brown

Meenakshi Upadhyaya



Available at: https://works.bepress.com/ajla_aksamija/137/

THERMOELECTRIC MATERIALS IN EXTERIOR WALLS

Experimental Study on Using Smart Facades for Heating and Cooling in High-Performance Buildings



Aja Aksamija, PhD
Department of Architecture, University of Massachusetts Amherst
aaksamija@umass.edu



Zlatan Aksamija, PhD
Department of Electrical and Computer Engineering, University of Massachusetts Amherst
zlatana@engin.umass.edu



Chris Counihan
Department of Architecture, University of Massachusetts Amherst
chris.counihan@gmail.com



Dylan Brown
Department of Architecture, University of Massachusetts Amherst
dtdylanb@gmail.com



Meenakshi Upadhyaya
Department of Electrical and Computer Engineering, University of Massachusetts Amherst
mupadhyaya@umass.edu

ABSTRACT

This article discusses design, prototype development and an experimental study of facade-integrated thermoelectric (TE) materials. TEs are smart materials that have the ability to produce a temperature gradient when electricity is applied, exploiting the Peltier effect, or to generate a voltage when exposed to a temperature gradient, utilizing the Seebeck effect. TEs can be used for heating, cooling, or power generation. In this research, heating and cooling potentials of these novel systems were explored. Initially, two low fidelity prototypes were designed and constructed, where one prototype was used to study integration of TE modules (TEM) as stand-alone elements in the facade, and one prototype was used to explore integration of TEMs and heat sinks in facade assemblies. Both prototypes were tested, in ambient conditions and within a thermal chamber. The thermal chamber was used to represent four different exterior environmental conditions (0°F, 30°F, 60°F and 90°F), while the interior conditions were kept constant at room temperature. The supplied voltage to facade-integrated TEMs varied from 1 to 8 V. Temperature outputs of TEMs for all investigated thermal conditions were measured using thermal imaging, which are discussed in detail in this article. The results indicate that while stand-alone facade-integrated TEMs are not stable, addition of heat sinks improves their performance drastically. Facade-integrated TEMs with heatsinks showed that they would operate well in heating and cooling modes under varying exterior environmental conditions.

KEYWORDS

Facade, intelligent, physical testing – mockups, fabrication prototypes, smart materials, heating and cooling, experimental, thermal imaging

INTRODUCTION

Buildings consume 40% of energy in the United States, and influence greenhouse gas emissions. High demand for energy used for lighting, heating, ventilation, and air conditioning leads to significant amount of carbon dioxide emissions. According to the U.S. Department of Energy, 15% of global electricity is consumed by various refrigeration and air-conditioning processes, and 46% of the energy used in household and commercial buildings is attributed to heating, ventilation and air-conditioning (HVAC) systems in 2011 (DOE, 2011). Given the high energy usage and inefficiencies found in conventional HVAC systems, new heating and cooling sources are needed in order to reduce buildings' carbon footprint. Moreover, integration of different building systems, particularly building envelope and HVAC, are essential for high-performance buildings. Thermoelectrics (TEs) are one example of a promising technology with potential architectural applications. Research and development has largely focused on thermoelectric modules (TEMs) that convert heat energy into electrical energy (Montecucco et al., 2012; Yilmazoglu, 2016) and novel TE materials that offer higher energy efficiency through nanoscale engineering (Snyder and Toberer, 2008). Heating and cooling modes can be switched by reversing the current direction (Fig. 1). TEMs can offer low cost electricity without the use of mechanical parts or production of toxic wastes (Seetaw et al., 2014). The optimal performance of TEMs depends on many factors, ranging from material selection to operation strategy (Twaha et al., 2016).

TEMs can be used for heating, cooling, or power generation (Fig. 2). TEMs consist of arrays of N and P type semiconductors. When a heat source is applied on one side of the semiconductor and the other side is exposed to a cooler temperature, electric power is produced (and can be generated in reverse). Electricity supply can actively provide cooling or heating by reversing the current direction (Zheng et al., 2014).

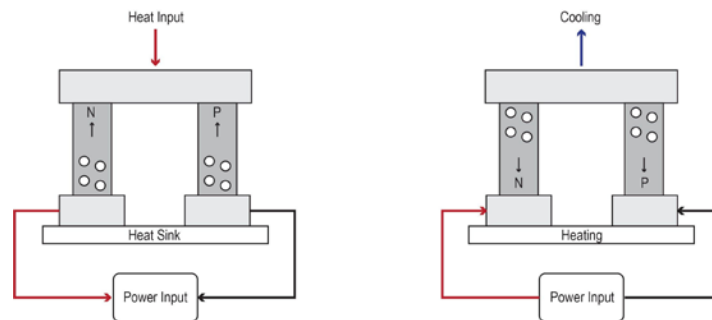


Figure 1: Thermoelectric materials produce electricity when exposed to thermal gradient, and cooling/heating when voltage is applied (Image by Authors).

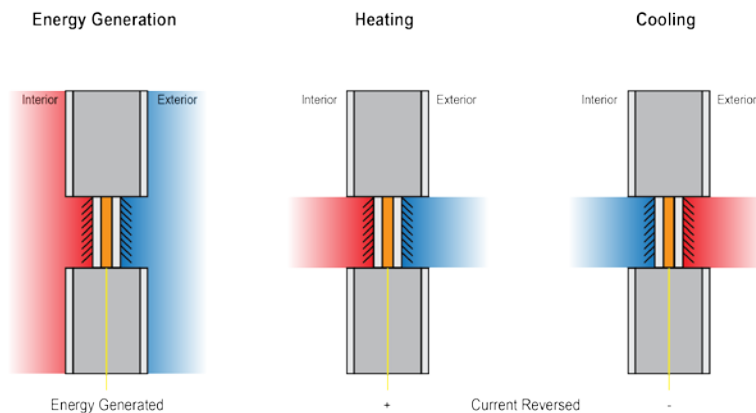


Figure 2: Potential use of TE materials in exterior walls for energy generation, heating and cooling (Image by Authors).

More recently, research on TE applications has gained momentum (Twaaha et al., 2016; Zhao and Tan, 2014). A promising, but not widely researched area, includes use of TE applications for heating and cooling, as well as energy generation.

BACKGROUND

In the past 15 years, significant growth of research into thermoelectric energy conversion is reflected in the increase in related annual publications, increasing from 500 to 2500 (Bell, 2008). TEMs have been used for cooling and heating applications in the military and aerospace fields, and for electronic instruments (Kraemer et al., 2011). Since TEMs do not contain any moving parts, their operation is quite reliable and stable. This greatly reduces maintenance costs when compared to other types of air conditioning systems (Shen et al., 2013). It is possible to use TEMs as an alternative to HVAC applications with properly designed heat exchangers (Yilmazoglu, 2016).

Research TEs began with Thomass J. Seebeck's 1821 discovery of the eponymous effect at a junction between two metals. In the 1950's, Ioffe and Goldsmid authored seminal works outlining the criteria for materials selection and optimization in TE modules. As a technology, TEs have a five-decades-long history dating back to early NASA deep-space probes, where they were used in conjunction with radioisotope heat sources to power satellites ranging from Pioneer 10 to Cassini as well as the Mars Rover (Ritz and Peterson, 2004). However, modest conversion efficiency (around 6-8%) limited the use of TEs to niche applications where robustness and reliability were more important than efficiency. In the past decade, global need for sustainable and renewable energy, coupled with advances in materials theory, simulation, and synthesis, have fueled a resurgence of interest in both materials discovery of more efficient TEMs and commercial applications in a variety of markets (Dresselhaus et al., 2007; Kanatzidis, 2010). Recent examples range from wearables such as the Matrix smart watch powered entirely by body heat to waste heat scavenging from car exhaust systems.

Thermoelectric heating and cooling has several advantages over conventional counterparts. The compact size, light weight, reliability, lack of mechanical parts and elimination of the need for chlorofluorocarbons make them environmentally friendly and appealing. But, applying thermoelectric systems for space heating and cooling remains much more challenging and has not been explored beyond small scale applications and in theoretical proposals (Zhao and Tan, 2014).

Few applications of TEMs in facade assemblies have been researched, proposed, or constructed. This has created a significant gap in knowledge in the potential architectural applications of TEMs. Some researchers, however, have proposed architectural applications with promising preliminary results. Liu et al. proposed a facade assembly that integrates TEM with a heat sink for heating and cooling needs. Results indicate that the total input power required to operate a TEM decreases as the distribution density of the TEMs increase. The thermal resistance of the heat sink plays an important role in determining the number of TE coolers optimizing all potential design configurations (Liu et al., 2015). This study proposed a window composed of four parts: a passive window, a PV module, thermoelectric cooling units, and heat sinks. A semi-transparent PV module is integrated into the front pane of a passive double-pane window and it is used to power TEMs integrated into the window frame. Finned heat sinks are placed in contact with the TE units to control the heat transfer between the TEMs and the ambient environment. The PV unit converts solar radiation into electrical energy, while the TEMs change this electrical energy into thermal energy. The TEMs can heat or a cool, depending on the direction of the current supplied by the PV unit. This would allow the building envelope to be used in both heating and cooling applications (Liu et al., 2015).

While the scientific principles and properties that govern TEs were discovered over one hundred years ago, the applications in facade systems have not been widely explored. This research addresses this gap in knowledge by investigating integration of TEMs into building facades for heating and cooling.

METHOD

The research questions that were addressed include:

- How can TEMs be integrated into architectural facade assemblies?
- How do TEMs behave in typical thermal conditions in various climates?
- How is TEM's thermal performance affected by varying voltages, climatic conditions and assembly construction?
- How is TEM performance affected by different configuration of heat sinks?

Two low fidelity TEM facade prototypes were designed and assembled for the purposes of this study. These were tested in

ambient and thermally controlled conditions to measure temperature gradients, heating and cooling potential. Materials for these assemblies were selected for their commercial availability, as well as their specifications. Two heat sink types were chosen to provide a comparison in heat transfer performance values.

The dimensions of TEM modules are 40mm x 40mm, drawing up to 12V, with operating conditions from -22°F to 181°F. Small heat sinks of 40mm x 40mm x 11mm, composed of aluminum cooling fins, were used to provide direct heat sinks for a flat heat sink assembly. These were fixed to the TEMs using 0.5mm silicone based thermal pads. The second prototype included larger heat sinks. Two 120mm heat sinks were used, with four direct heat copper pipes for heat dissipation. Thermal paste provided a thermal connection to the TEM module.

Five configurations were considered when constructing prototypes for testing (Fig. 3). A direct contact TEM facade module would provide the simplest assembly, applying heat sinks directly to the TEM. This assembly, however, poses the greatest potential for thermal bridging and gaps in the facade assembly. A sink transfer assembly expands upon the direct contact assembly, but relies on conductors to transfer heat from the TEM to heat sinks. Location shift assemblies are similar to sink transfer assemblies, but allow for flexibility in regards to heat sink location in relation to the TEM. Stacked TEMs provide the opportunity to increase the temperature differences between the hot and cold sides beyond what is possible with a single TEM across multiple modules. Floor mounted assemblies consider integrating TEMs, conductors, and heat sinks into the floor plate and facade. This assembly is the most complicated application, but provides benefits that include natural convection and heat sink concealment.

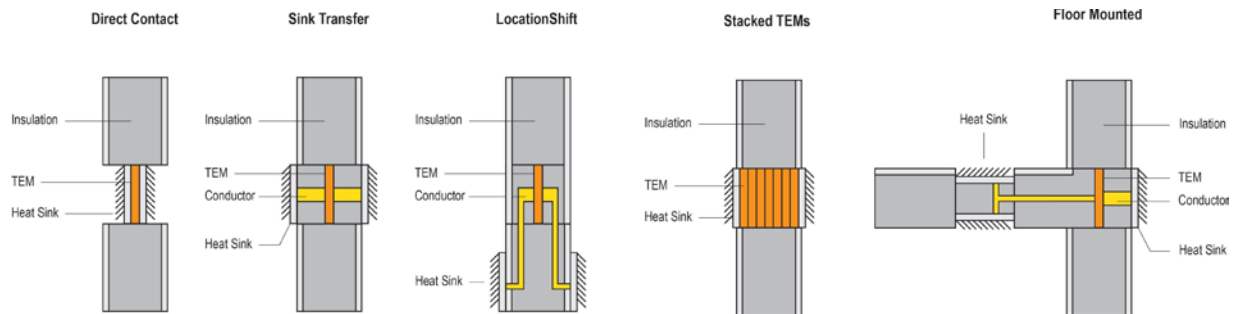


Figure 3: Schematic representation of possible configuration and placement of TEMs in facades (Image by Authors).

For the purposes of this research, direct contact and sink transfer TEM facade assemblies were selected, for their simplicity and broad applicability. Each assembly was constructed using 2, 1" foam insulation panels with an R-value of 5, providing each assembly with an R-value of 10. Thin board (1/8") was glued to face the foam insulation and provided a housing within the assembly for the TEM modules and heat sinks. Heat sinks were inserted into the assembly and connected to the TEM using thermal paste or thermal pads. The flat assembly did not rely on any fasteners to connect the TEMs to the heat sinks, instead thermal pads provided the adhesion. The large heat sink assembly required an assembly composed of nuts, bolts, and washers to sandwich the TEM, foam, and board assembly together. Spray foam insulation was applied to the larger heat sink assembly to prevent any thermal breaks that may have developed through use of metal hardware and fasteners. These assemblies can be seen in Figures 4 and 5.

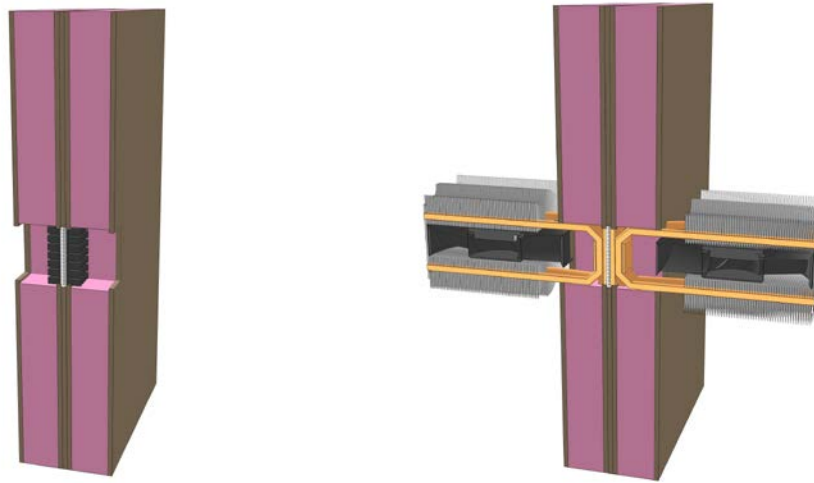


Figure 4: Architectural TEM proof of concept assembly model sections (Image by Authors).

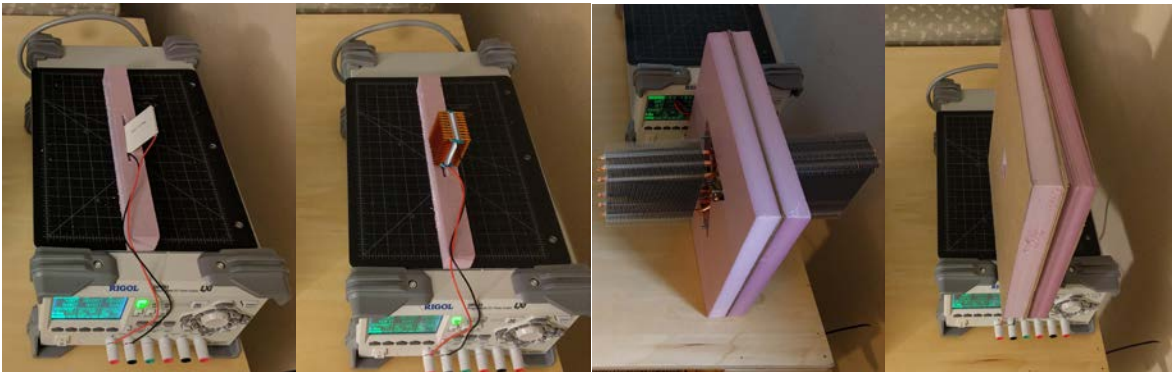


Figure 5: TEM proof of concept mockups (Image by Authors).

To understand how facade-integrated TEMs behave, these prototypes were first tested in ambient room conditions (temperature of 72°F). An independent module without a heat sink, a module with a flat heat sink, as well as the assembly mockups were tested with applied voltage of 1V increments. Results were measured using thermal imaging camera, as well as a power supply. Thermal images were taken at one volt increments up to 8V, and temperatures were recorded using thermal camera.

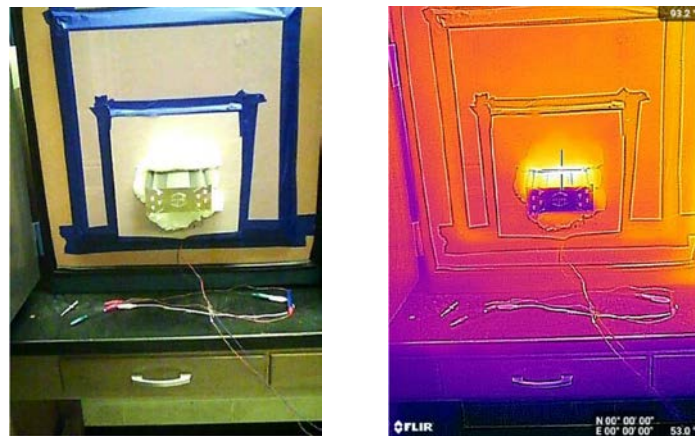


Figure 6: TEM assembly testing in thermal chamber with thermal imaging (Image by Authors).

Further testing involved the use of a temperature controlled thermal chamber. The thermal chamber's 16.5" x 16.5" opening was sealed using 1" of insulating foam with tape applied to provide a relatively air tight seal for the testing. Assemblies were inserted into a 10"x10" void and were taped again (Fig. 6). The 10"x10" void allowed for easy insertion and removal of the prototypes. The chamber was set to 0°, 30°, 60°, and 90°F to represent different exterior temperatures (winter, summer and intermediate seasons). This method of testing simulated typical exterior temperatures found in most climates while allowing for temperature data to be collected in a controlled setting. The thermal chamber was allowed time to stabilize (1 hr) before each testing session, and 20 minute breaks were taken in between each observation. The ambient temperature of the room was kept relatively stable at 73°F. Voltage was applied in 1 V increments in both heating and cooling modes. Temperature measurements on the exterior surface of the prototypes were recorded using a thermal camera.

RESULTS

AMBIENT TESTING RESULTS

Results were collected, tabulated, and graphed for analysis. The temperatures observed in ambient testing ranged from 48.8°F to 258.3°F in both cooling and heating modes. The maximum temperature observed occurred on the hot side of the flat heat sink at 8V. The independent TEM approached this value, reaching 238.2°F at 6V before module failure. Heating side maximums exceeded 200°F in all ambient assembly tests, except for the large heat sink (measured temperature for of this assembly was 98.3°F at 8V). All heating side temperatures show positive temperature trends (Fig. 7).

Cooling temperatures displayed inconsistent data. Temperatures ranged from 48.8°F to 181.1°F. Cold side temperatures elevate significantly on the independent TEM, flat heat sink, and flat heat sink assembly above 4V. The cold side temperatures of these testing modules exceed 100°F at or around 4V. The large heat sink shows temperatures ranging from 59.5°F to 48.8°F. The temperature difference and average temperature values were the lowest for this assembly.

Modules without heat sinks were stressed by high temperature difference values, often times exceeding those suggested by the manufacturer. Average temperatures show similar stresses, and can reach or exceed 200°F. TEM failures occurred on several occasions, most notably when TEMs were not paired with heat sinks, or if voltages exceeded 8V. Only the large heat sink maintained a stable average temperature, stressing the importance of incorporating a heat sink for the proper functioning of facade-integrated TEMs.

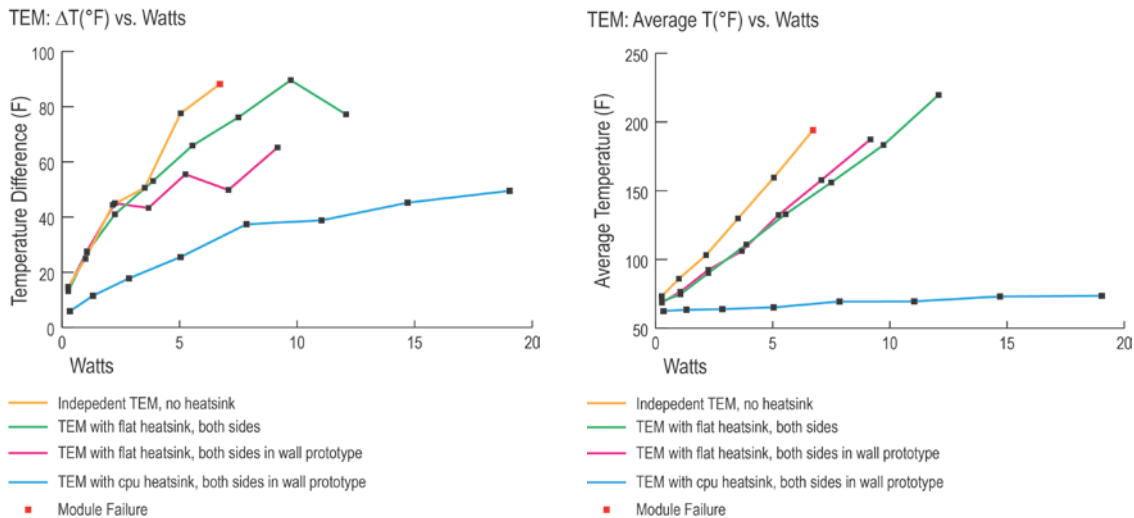


Figure 7: Temperature difference and average temperature results in ambient conditions (Image by Authors).

Temperature difference data indicates that a threshold of failure exists within the TEM module, occurring around 80°F, 15°F above the manufacturer's stated value. When plotted against power, the data show performance in line with observations, indicating that the temperature differentials were directly influenced by the presence of a heat sink. Data also shows that heat sinks allow a higher power input without leading to extreme temperature differentials.

THERMAL CHAMBER TESTING RESULTS: HEATING

Results of the thermal chamber testing indicate that the temperature values increase as higher voltages are applied, regardless of the assembly type or tested temperature (Fig. 8). The results for the prototype with a large heat sink show that temperatures range from 56.4°F to 97.1°F when applied in 1V increments. Tested temperature of 0°F yields a heating temperature range of 66.9°F to 80.1°F. Observed values start at 66.9°F due to the ambient temperatures of the testing room. Values always remained above 0°F temperature. 30°F ambient temperature data show values rising from 56.4°F to 81.6°F from 1V to 5V respectively. At 6V, a decline in temperature to 75.8 was observed. At 60°F ambient temperature, heat sink values ranged from 73.8°F to 97.1°F. Temperatures rose relatively consistently at this tested temperature.

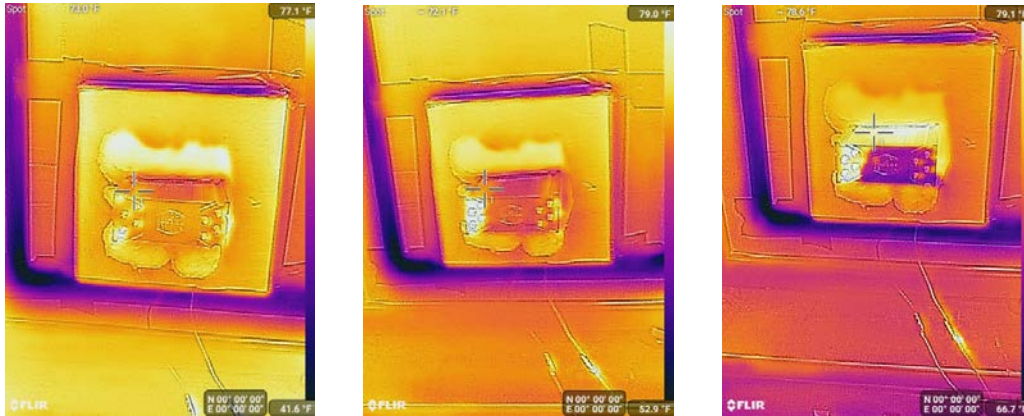


Figure 8: Assembly heating at 0, 30, 60°F with 3V applied.

Heating performance of the assembly with flat heat sink shows temperatures ranging from 28.8°F to 177°F. The heating from this assembly always exhibits a positive trend with increasing voltage. At 0°F temperature, heating temperatures range between 28.8°F to 80.6°F. Observed values without applied voltage start at 26.6°F. At 30°F temperature, results show values rising from 49.6°F to 159.8°F from 1V to 6V respectively. At 60°F temperature, values ranged from 70.5°F to 177°F. Heat sink temperatures at this temperature exceeded 100°F when 3V is applied.

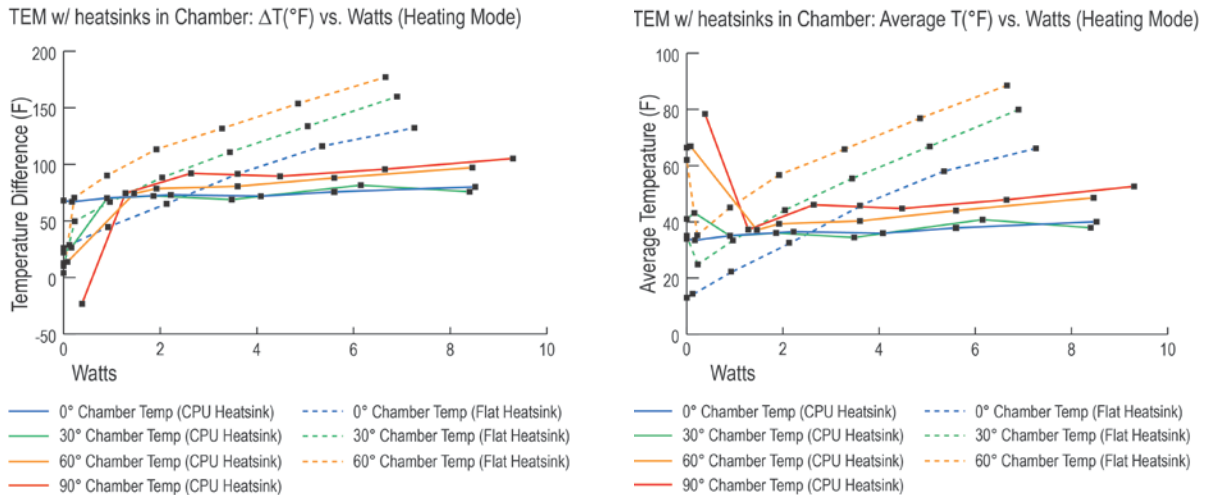


Figure 9: ΔT vs Watts and average temperature vs Watts in heating mode (Image by Authors).

Temperature difference data in the heating mode indicates that heating performance behaves consistently despite thermal chamber temperatures (Fig. 9). Higher thermal chamber temperatures lead to higher temperature differences with increasing power being applied. This was observed in both assemblies; however, the flat heat sink showed positive trends, while the large heat sink showed relatively constant temperature differences with increasing power. The temperature differences observed in the flat heat sink greatly exceeded the manufacturer stated maximum of 65°F, leading to failure at 7W. The large

heat sink assembly displayed a relatively constant difference of 65-70°F, even as power input increases.

THERMAL CHAMBER TESTING RESULTS: COOLING

TEM cooling data shows temperature values that are dependent on TEM assembly. The large heat sink data show that at a 60°F ambient temperature, cooling ranges from 71.6°F to 46.1°F when voltage is applied in 1V increments. However, cooling does not occur linearly. The minimum temperature was observed when 4V was applied to the large heat sink, while 5V and 6V values were slightly higher, at 53.7°F and 49.5°F respectively. Cooling performance was more effective at 60°F. Temperatures observed at 1-3V were higher than 60°F temperature (due to testing room temperature), but lowered significantly when higher voltages were applied. At 90° temperature, TEM performance is relatively uniform. Measured temperatures ranged from 57.2°F to 66.8°F.

The flat heat sink assembly showed results ranging from 43.3°F to 93.9°F. Observed temperatures were lower when operated at a 60°F temperature, and remained below the ambient temperature through 4V. Temperatures observed at 90°F ranged from 72.8°F to 93.9°F. Temperatures remained below the ambient temperature up to 5V, but temperatures observed would not provide adequate cooling for occupant thermal comfort.

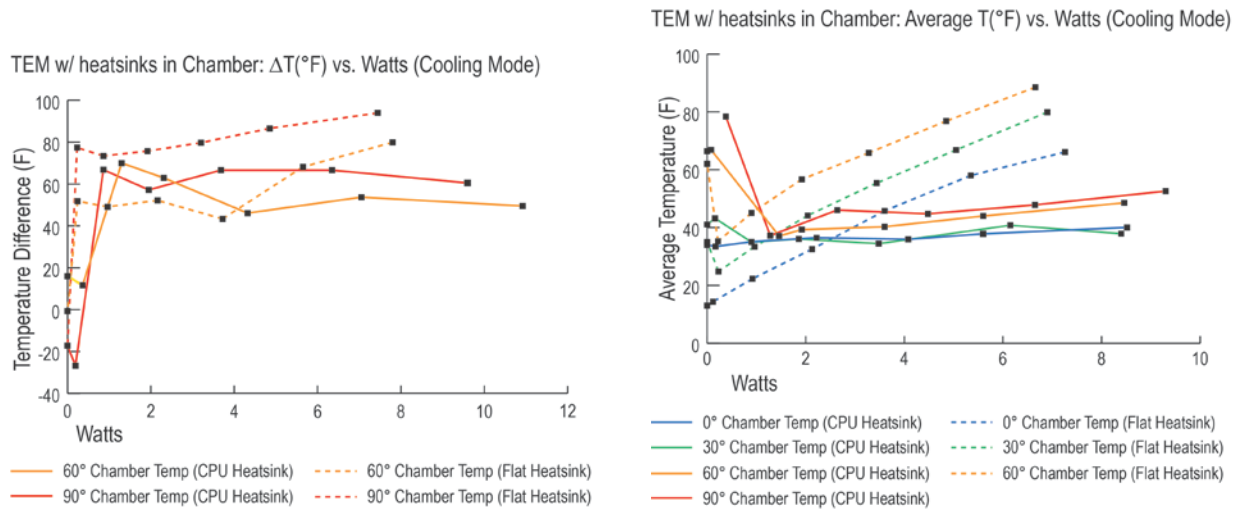


Figure 10: ΔT vs Watts and average temperature vs Watts in cooling Mode (Image by Authors).

Results for the cooling mode indicates that higher temperature differences arise as power inputs increases within the assemblies (Fig. 10). This was observed in both assemblies; however, the flat heat sink showed positive trends, while the large sink showed a slightly negative trend or constant temperature difference trend.

DISCUSSION

The results show that TEMs operate at effective heating and cooling temperatures even when exposed to variable exterior temperatures, represented by the thermal chamber. They are most effective when paired with a larger heat sink, especially for cooling. Results also show that TEMs, when integrated into facade prototypes, operate effectively in heating and cooling modes.

Data shows that the TEMs are more effective for heating and cooling applications when paired with heat sinks. Data also shows that when TEMs are paired with a larger heat sink, the cooling side operates more efficiently, and is affected to a lesser extent by temperatures generated within the TEM and any thermal bridging that may be occurring across the TEM.

The heating and cooling functions of TEMs appear to be most effective and efficient for cooling operations when 2-4V are applied to the module. This effect is more evident in the small heat sink assembly, whereas the larger heat sink assembly maintains a more consistent temperature as voltage above 3V is applied.

TEM modules operating without a heat sink or with a small heat sink are inefficient or ineffective. Without a means to transport and dissipate heat, TEM modules overheat due to the thermal transport involved at the molecular level. Thermal bridging may also contribute to high cold side temperatures.

CONCLUSION AND FUTURE WORK

Results of this study show promising opportunities for integrating TEMs in facade systems, since these smart materials can be used for heating and cooling of interior spaces. The performance of facade-integrated TEMs is most useful when paired with a larger heat sink, especially for the purposes of heating. This assures adequate heat dissipation from these advanced materials. TEM modules operating without a heat sink or with a small heat sink are inefficient. Results indicate that stand-alone facade-integrated TEMs are not stable, and are not promising for architectural heating and cooling needs. Without a means to transport heat, TEM modules overheat due to the molecular thermal transport within the modules. However, facade integrated TEMs paired with heat sinks displayed effective heating and cooling operation under varying exterior environmental conditions.

Integrated TEM facades offer many potential benefits. The mechanical equipment required for HVAC can be reduced, leading to lower maintenance requirements and operational cost reductions. TEMs can be integrated and paired with radiant panels to cause less disruption to interior spaces than traditional HVAC equipment. Finally, TEMs do not require moving parts or refrigerants for heating and cooling, thus improving environmental impact of HVAC systems.

Next steps for this research will include investigation of thermal transport in several different exterior wall types (computational and experimental), used for commercial and residential applications. Actual wall assemblies will be investigated, including rainscreen applications, light-wood framed walls and curtain walls. Also, efficiencies and impact on energy consumption will be studied, and the results will be reported in future publications.

REFERENCES

- Bell, L. "Cooling, heating, generating power, and recovering waste heat with thermoelectric systems." *Science* 321 (2008): 57–61.
- Department of Energy. "Building Energy Data Book 2011." <https://openei.org/doe-opendata/dataset/buildings-energy-data-book> (accessed March 30, 2017).
- Dresselhaus, M., Chen, G., Tang, M., Yang, R., Lee, H., Wang, D., Ren, Z., Fleurial, J., and Gogna, P. "New directions for low-dimensional thermoelectric materials." *Advanced Materials* 19 (2007):1043–1053
- Kanatzidis, M. G. "Nanostructured thermoelectrics: the new paradigm?" *Chemistry of Materials* 22 (2010): 648–659.
- Kraemer, D., Poudel, B., Feng, H., Caylor, J., Yu, B., Yan, X., Ma, Y., Wang, X., Wang, D., Muto, A., McEnaney, K., Chiesa, M., Ren, Z., and Chen, G. "High-performance flat-panel solar thermoelectric generators with high thermal concentration." *Nature Materials* 10 (2011): 532-538.
- Liu, Z. B., Zhang, L., Gong, G., and Luo, Y. "Evaluation of a prototype active solar thermoelectric radiant wall system in winter conditions." *Applied Thermal Engineering* 89 (2015): 36-43.
- Montecucco, A., Buckle, J. R., and Knox, A. R., "Solution to the 1-D unsteady heat conduction equation with internal Joule heat generation for thermoelectric devices." *Applied Thermal Engineering* 35 (2012): 177–184.
- Ritz, F. and Peterson, C. "Multi-mission radioisotope thermoelectric generator (MMRTG) program overview." *Proceedings of the 2004 IEEE Aerospace Conference* (2004): 2950-2957.
- Seetawan, T., Singsoog, K., and Srichai, K. "Thermoelectric energy conversion of p-Ca₃Co₄O₉/n-CaMnO₃ module." *Proceedings of the 6th International Conference on Applied Energy* (2014): 2–5.
- Shen, L., Xiao, F., Chen, H., and Wang, S. "Investigation of a novel thermoelectric radiant air-conditioning system." *Energy and Buildings* 59 (2013): 123-132.
- Snyder, G. and Toberer, E. "Complex thermoelectric materials." *Nature Materials* 7 (2008): 105-114.
- Twaha, S., Zhu, J., Yan, Y., and Li, B. "A comprehensive review of thermoelectric technology: Materials, applications, modelling and performance improvement." *Renewable and Sustainable Energy Reviews* 65 (2016): 698-726.
- Yilmazoglu, M. "Experimental and numerical investigation of a prototype thermoelectric heating and cooling unit." *Energy and Buildings* 113 (2016): 51-60.
- Zheng, X.F., Liu, C. X., Yan, Y. Y., and Wang, Q. "A review of thermoelectrics research - recent developments and potentials for sustainable and renewable energy applications." *Renewable Sustainable Energy* 32 (2014): 486–503.
- Zhao D., and Tan G. "A review of thermoelectric cooling: Materials, modeling and applications." *Applied Thermal Engineering* 66 (2014): 15-24.